

CALCULATION OF THE TEMPERATURE FIELD OF A ZONE-REFINED SILICON ROD

Yu. E. Nedzvetskii, D. G. Ratnikov, N. A. Avdonin, and B. Ya. Martuzan

Inzhenerno-Fizicheskii Zhurnal, Vol. 13, No. 2, pp. 225-231, 1967

UDC 621.785.1

A problem closely approximating the actual physical conditions of the silicon zone refining process is formulated mathematically. Certain calculation results are presented. These are compared with experimental data on the principal characteristics of the process.

In zone refining, the temperature distribution in the rod controls the most important characteristics of the refining process itself and predetermines the properties of the single crystal produced. The distribution of electrical properties over the crystal cross section depends on the configuration of the crystallization front. The temperature gradients in the rod near the crystallization front are associated with the conditions of dislocation growth. Moreover, the relative position and configuration of the crystallization and fusion fronts determine the zone height necessary to melt through the rod, etc.

This paper presents a method and certain results of solving the three-dimensional problem of heat conduction with allowance for the heat of crystallization using the closest possible approximation of the boundary conditions to the actual characteristics of induction zone refining. We chose silicon as our experimental material because of its commercial importance.

The object of the calculations is to construct the temperature field under various melting conditions and determine the effect of the zone refining conditions on the more important characteristics of the process. Special attention is given to the determination of the shape of the crystallization and fusion fronts and to the determination of the temperature in the part of the

solid rod where the silicon is plastic (temperature region above 900°C).

Under the initial conditions of the problem, the silicon rod is assumed to be an infinitely long, straight, circular cylinder of radius R moving at constant ve-

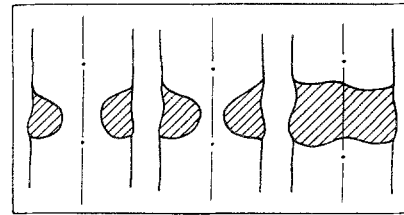


Fig. 2. Melting zones at various heating powers. R = 1.5 cm, v = 0. Experimental data.

locity v. The integral radiation factor σ , the specific heat c, and the density ρ are assumed constant and independent of the temperature and state of aggregation of the silicon. The thermal conductivities of the solid λ_s and liquid λ_l phases are also assumed constant.

In what follows:

1) The temperature distribution in the rod is described by the heat-conduction equation, a certain effective thermal conductivity λ_l being given in the liquid phase. The choice of this coefficient makes it possible to take into account to some extent convective

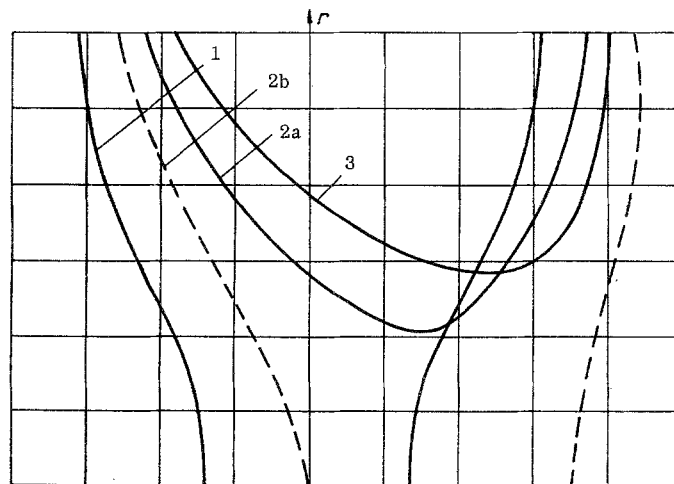


Fig. 1. Steady-state fusion and crystallization isotherms for R = 1 cm, P = 850 W at various velocities v. Theoretical data: 1) v = 0; k = 1; 2a) v = 5 mm/min; k = 1; 2b) v = 5 mm/min; k = 100; 3) v = 10 mm/min; k = 1.

mixing in the liquid phase. Let $T(\bar{r}, \bar{z}, \bar{t})$ be the temperature of the rod at the point (\bar{r}, \bar{z}) at time \bar{t} . Then in the moving coordinate system (\bar{r}, \bar{z}) tied to the

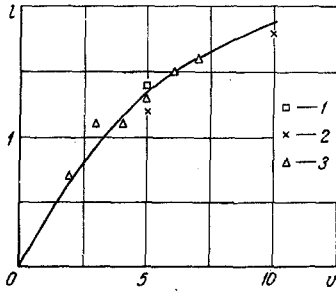


Fig. 3. Effect of zone velocity v (mm/min) on displacement l of the zone (mm) relative to the inductor: 1) calculation date for $\lambda_1/\lambda_s = 1$; 2) the same for $\lambda_1/\lambda_s = 100$; 3) experimental data.

moving rod the heat-conduction equation for a cylinder of radius R is written as

$$\lambda(T) \left(\frac{\partial^2 T}{\partial \bar{r}^2} + \frac{1}{\bar{r}} \frac{\partial T}{\partial \bar{r}} + \frac{\partial^2 T}{\partial \bar{z}^2} \right) = c \rho \frac{\partial T}{\partial \bar{t}},$$

$$\bar{t} > 0; \quad 0 < \bar{r} < R; \quad -\infty < \bar{z} < \infty,$$

$$\lambda(T) = \begin{cases} \lambda_s, & T < T_f, \\ \lambda_l, & T > T_f. \end{cases} \quad (1)$$

2) Assuming radiation according to the Stefan-Boltzmann law and surface power sources created by a stationary inductor, we write the conditions at the surface of the rod as

$$-\lambda(T) \frac{\partial T}{\partial \bar{r}} = \sigma T^4 - \Phi(\bar{z} + v\bar{t}) \quad (2)$$

at $\bar{r} = R$.

3) In accordance with the theory and practice of induction heating [1], the power sources Φ are assumed to be distributed over the surface with density

$$\Phi(s) = \frac{P}{2\pi R} \times \frac{\left[\operatorname{arctg} \frac{s+0.5a}{d} - \operatorname{arctg} \frac{s-0.5a}{d} \right]^2}{\int_{-\infty}^{\infty} \left(\operatorname{arctg} \frac{s+0.5a}{d} - \operatorname{arctg} \frac{s-0.5a}{d} \right)^2 ds} \quad (3)$$

4) The liberation and absorption of the heat of phase transition at the solid-liquid phase interface are described by the Stefan condition

$$\gamma \rho \frac{\partial \varphi}{\partial \bar{t}} + (\lambda(T) \operatorname{grad} T)_{T=T_f}^{\bar{r}=T_f^-} - \operatorname{grad} \varphi = 0, \quad (4)$$

γ is the specific latent heat of crystallization; $\varphi(\bar{r}, \bar{z}, \bar{t}) = 0$ is the surface equation of the isotherm $T = T_s$;

$(\lambda(T) \operatorname{grad} T)_{T=T_f}^{\bar{r}=T_f^-}$ denotes the jump in the quantity $\lambda(T) \operatorname{grad} T$ on crossing the surface $T = T_f$.

To Eqs. (1)–(4) we must add the conditions

$$T(\bar{r}, \bar{z}, \bar{t}) \text{ is bounded at } \bar{r} = 0,$$

$$\frac{\partial T}{\partial \bar{z}} = 0 \text{ as } |\bar{z}| \rightarrow \infty. \quad (5)$$

We introduce the fixed coordinate system (\bar{r}, \bar{x}) tied to the stationary inductor:

$$\bar{r} = \bar{r}; \quad \bar{x} = \bar{z} + v\bar{t}.$$

In addition, we introduce the following dimensionless quantities:

$$r = \frac{\bar{r}}{R}; \quad z = \frac{\bar{z}}{R}; \quad x = \frac{\bar{x}}{R}; \quad t = \frac{\lambda_s \bar{t}}{c \rho R^2};$$

$$\mu = \frac{c \rho R}{\lambda_s} v; \quad x = z + \mu t;$$

$$u = \frac{1}{k(u)} \cdot \frac{T - T_f}{T_f - T_0}; \quad k(u) = \begin{cases} 1, & u < 0, \\ \frac{\lambda_s}{\lambda_l}, & u > 0. \end{cases}$$

We also assume that the rod is not infinitely long but bounded by the coordinates $x = -B$, $x = B$.

Then conditions (1)–(5) reduce to the following dimensionless form

$$\frac{\partial^2 u}{\partial r^2} + \frac{1}{r} \frac{\partial u}{\partial r} + \frac{\partial^2 u}{\partial x^2} = c(u) \left(\mu \frac{\partial u}{\partial x} + \frac{\partial u}{\partial t} \right),$$

$$t > 0; \quad 0 < r < 1; \quad -B < x < B, \quad (6)$$

$$\frac{\partial u}{\partial r} = \alpha \Phi(Rx) - \beta [k(u)u + \delta_1]^4 \text{ at } r = 1, \quad (7)$$

$$\frac{\partial u}{\partial x} = 0 \text{ at } |x| = B, \quad (8)$$

u is bounded at $r = 0$.

Here

$$\alpha = \frac{R}{\lambda_s (T_f - T_0)}; \quad \beta = \frac{\sigma R (T_f - T_0)^3}{\lambda_s}; \quad \delta_1 = \frac{T_f}{T_f - T_0}.$$

Equation (6) has been written in a form suitable for application of the "through calculation" method described in [2]. In this case on the right side of Eq. (6) there appears the term

$$\frac{\partial a(u)}{\partial t} + \mu \frac{\partial a(u)}{\partial x}$$

with the discontinuous coefficient $a(u)$ resulting from the Stefan condition (4). Smoothing of the coefficient $a(u)$ by the method proposed by Oleinik [3] leads to the following value of the coefficient $c(u)$:

$$c(u) = \begin{cases} 1, & u < L, \\ \frac{b}{2L} + 0.5 \left(1 + \frac{\lambda_s}{\lambda_l} \right), & |u| < L, \\ \frac{\lambda_s}{\lambda_l}, & u > L. \end{cases} \quad (9)$$

Here, $b = \gamma c^{-1}(T_f - T_0)^{-1}$ and L is a small number which may be arbitrarily selected. The choice of L depends on the accuracy of approximation of the Stefan condition at the phase interface.

Although we are interested only in the stationary temperature distribution $u(r, x)$, we will deliberately retain the term with $\partial u / \partial t$ in Eq. (6).

Below we make use of the method of solving a stationary problem by solving the corresponding nonstationary problem, in this case (6)–(8), until a steady state is reached. For this purpose we employ one of the economical variable-direction finite-difference schemes using one-dimensional pivots in each direction. We introduce the difference net with space nodes at the points (x_i, r_j) and time nodes at the points t_k , where $i = 0, 1, 2, \dots, M$; $x_0 = -B$, $x_M = B$; $j = 0, 1, 2, \dots, N$; $r_0 = 0$, $r_N = 1$; $k = 0, 1, 2, \dots$; $t_0 = 0$.

We replace Eq. (6) by its finite-difference equivalent, using a scheme similar to that proposed in [4]:

$$\begin{aligned} \frac{c_{ij}^k}{\tau_k} \left(u_{ij}^{k+\frac{1}{2}} - u_{ij}^k \right) &= \frac{2 u_{i+1j}^{k+\frac{1}{2}}}{h_{i+1}(h_i + h_{i+1})} + \frac{2 u_{i-1j}^{k+\frac{1}{2}}}{h_i(h_i + h_{i+1})} - \\ &- \frac{2 u_{ij}^{k+\frac{1}{2}}}{h_i h_{i+1}} - \frac{\mu c_{ij}^k}{h_i + h_{i+1}} \left(u_{i+1j}^{k+\frac{1}{2}} - u_{i-1j}^{k+\frac{1}{2}} \right) + \\ &+ \frac{1}{g^2} (u_{ij-1}^k - 2 u_{ij}^k + u_{ij+1}^k) + \\ &+ \frac{1}{2 g r_j} (u_{ij+1}^k - u_{ij-1}^k), \end{aligned} \quad (10)$$

$$\begin{aligned} \frac{c_{ij}^{k+\frac{1}{2}}}{\tau_k} \left(u_{ij}^{k+1} - u_{ij}^{k+\frac{1}{2}} \right) &= \frac{1}{g^2} (u_{ij-1}^{k+1} - 2 u_{ij}^{k+1} + \\ &+ u_{ij+1}^{k+1}) + \frac{1}{2 g r_i} (u_{ij+1}^{k+1} - u_{ij-1}^{k+1}) + \frac{2 u_{i+1j}^{k+\frac{1}{2}}}{h_{i+1}(h_i + h_{i+1})} + \\ &+ \frac{2 u_{i-1j}^{k+\frac{1}{2}}}{h_i(h_{i+1} + h_i)} - \\ &- \frac{2 u_{ij}^{k+\frac{1}{2}}}{h_i h_{i+1}} - \frac{\mu c_{ij}^{k+\frac{1}{2}}}{h_i + h_{i+1}} \left(u_{i+1j}^{k+\frac{1}{2}} - u_{i-1j}^{k+\frac{1}{2}} \right). \end{aligned} \quad (10^1)$$

Here, $u_{ij}^k = u(x_i, r_j, t_k)$; $c_{ij}^k = c(u_{ij}^k)$; $h_i = x_i - x_{i-1}$; $g_j = r_j - r_{j-1}$; $\tau_k = t_k - t_{k-1}$.

We first calculate values of the function $u_{ij}^{k+1/2}$ on the half-step, and then values of the function u_{ij}^{k+1} on the full step. In this case on the half-step the derivatives with respect to x are implicitly, and the derivatives with respect to r explicitly, approximated; conversely, on the full step the derivatives with respect to x are explicitly, and those with respect to r implicitly, approximated.

This makes it possible to use one-dimensional pivot formulas at each half-step and step [5]. Boundary condition (7) at the surface $r = 1$ is approximated as follows:

$$\begin{aligned} \frac{1}{g} (u_{iN}^{k+1} - u_{iN-1}^{k+1}) &= \alpha \Phi(Rx_i) - \\ - \beta [k(u_{iN}^k) u_{iN}^{k+1} + \delta_1] [k(u_{iN}^k) u_{iN}^k + \delta_1]^3. \end{aligned} \quad (11)$$

On the axis of the rod $r = 0$ we impose the requirement $\lim_{r \rightarrow 0} \frac{\partial u}{\partial r} = 0$, so that

$$\lim_{r \rightarrow 0} \frac{1}{r} \frac{\partial u}{\partial r} = \frac{\partial^2 u}{\partial r^2}.$$

With this remark in mind, we approximate Eq. (6) on the line $r = 0$ in the usual way. A total of 80 nodes was taken over the entire interval of variation of x : $-B < x < B$. The steps h_i were varied over the total number of nodes. This made it possible to select the parameter B so that the restriction on the length of the rod did not lead to a serious distortion of the isotherm profile in the region affected by the inductor. In the final analysis the interval of variation of x from -13.5 to $+13.5$ was divided by points as follows:

$$\begin{aligned} h_0 &= h_1 = \dots = h_5 = 1.0, \\ h_6 &= h_7 = \dots = h_{15} = 0.5, \\ h_{16} &= h_{17} = \dots = h_{21} = 1/6, \\ h_{22} &= h_{23} = \dots = h_{57} = 1/12, \\ h_{58} &= h_{59} = \dots = h_{63} = 1/6, \\ h_{64} &= h_{65} = \dots = h_{73} = 0.5, \\ h_{74} &= h_{75} = \dots = h_{79} = 1.0. \end{aligned}$$

The step with respect to r was assumed constant, $g = 1/12$. In approximating the Stefan condition (expression for the coefficient $c(u)$) we varied the parameter L . In the final analysis we took $L = 0.0125$.

For an optimum choice of time steps τ_k the machine time required to calculate one variant of the problem was 80–90 min (BESM-2M computer).

In carrying out the computations it was assumed that the steady state had been reached when the maximum difference in the values of u in two successive time steps did not exceed 0.00001. In order to find the shape of the zero isotherm (fusion and crystallization isotherms) we carried out linear interpolation between two adjacent nodes of the net. This introduced an additional error in determining the isotherms.

We present the results of the calculations for several variants. The calculations were made for a silicon rod. The common values of the parameters were as follows: $a = 0.4 \cdot 10^{-2}$ m; $d = 0.5 \cdot 10^{-2}$ m; $\lambda_S = 30$ W/m·deg; $c = 960$ W·sec/kg·deg; $\rho = 2300$ kg/m³; $\gamma = 1.8$ J/kg; $\sigma_0 = 3.12 \cdot 10^{-8}$ J/m²·deg⁴·sec; $T_f = 1420^\circ$ C; $T_0 = 20^\circ$ C.

Figure 1 shows the isotherms $u = 0$ found for the variant $R = 0.01$ m, $P = 850$ W at different velocities v ($v = 0, 0.83 \cdot 10^{-4}$, and $1.67 \cdot 10^{-4}$ m/sec).

The figure shows the qualitative variation of the fusion region and the zone height at the surface of the rod as the velocity v changes. At $v = 0.83 \cdot 10^{-4}$ m/sec the isotherms are given for $k = \lambda_1 / \lambda_S = 1$ and for $k = 100$. Variation of the thermal conductivity in the liq-

uid phase is seen to have a strong influence on the position of the isotherm.

The calculated results were checked experimentally. In a first series of experiments we investigated the relationship between the zone height and the configuration of the isothermal surfaces for a stationary zone.

The check depended upon determination of the configurations of the crystallization and fusion surfaces which were established by blowing off the melt with a powerful gas jet and simultaneously switching off the melting generator. Melting was carried out in air after first determining that this would have only a slight effect on the results as compared with vacuum conditions. The experiments were performed on rods of technical silicon 0.03 m in diameter and 0.2 m long. The molten zone was created in the middle of the rod which eliminated the distorting influence of heat flow into the end grips. There was no displacement of the zone along the rod.

The results obtained are presented in Fig. 2. Approximately plane fusion surfaces were obtained at the same zone height as determined theoretically for $v = 0$.

In this connection, however, it is not correct to speak of total similarity of the temperature fields obtained by calculation and experiment. For example, in the theory the directional displacement of particles of liquid silicon observed under actual zone refining conditions was not taken into account.

In the second series of experiments we investigated the effect of the latent heat of fusion, associated with motion of the zone, and the specific heat on the displacement of the zone relative to the inductor.

By the displacement l we understand the displacement of the middle of the molten zone on the surface relative to the position of the inductor.

The experiments were carried out in a vacuum. The displacement was determined by projecting an enlarged image of the zone on a screen. The results of the experiments are presented in Fig. 3.

A comparison of theory and experiment also shows that calculations at $\lambda_l/\lambda_s = 100$ give much better agreement with experiment.

In conclusion, it may be stated that the experimental verification of the calculations confirms the possibility of theoretically predicting the shape of the fusion

isotherms and other qualitative characteristics of the zone refining process as a function of the process parameters.

On the basis of a theoretical solution of the zone refining problem it is possible to solve the problem of the optimal choice of process parameters (P, v) giving the best qualitative characteristics (for example, choice of the power P giving the flattest crystallization front).

Work of this nature is now being carried out at the All-Union Scientific Research Institute of High-Frequency Currents in collaboration with the Computer Center of the Latvian State University and will be the subject of a subsequent communication.

NOTATION

Here R is the radius of the rod; v is the velocity of the rod; σ is the integral radiation factor; c is the specific heat; ρ is the density; λ_s and λ_l are the thermal conductivities of the solid and liquid phases, respectively; T is the temperature; T_f is the melting (fusion) point of the rod material; T_0 is the ambient temperature; γ is the specific latent heat of crystallization; P is the total power of the inductor, a is the width of the inductor; d is the gap between the inductor and the rod.

REFERENCES

1. G. I. Babat, *Induction Heating of Metals and Its Industrial Application* [in Russian], 1965.
2. S. L. Kamenomostskaya, *Mat. sb.*, **53**, no. 4, 1961.
3. O. A. Oleinik, *DAN SSSR*, **135**, no. 5, 1960.
4. D. W. Peaceman and H. H. Rachford, *I. Soc. Indust. Appl. Math.*, **3**, no. 1, 1955.
5. I. S. Berezin and N. P. Zhidkov, *Methods of Computation* [in Russian], **2**, 1959.

16 November 1966

Vologdin Institute of High-Frequency Currents, Leningrad

Petr Stuchka Latvian State University Computer Center, Riga